HHS Public Access

Author manuscript

J Mater Chem B Mater Biol Med. Author manuscript; available in PMC 2018 January 07.

Published in final edited form as:

J Mater Chem B Mater Biol Med. 2017 January 7; 5(1): 151–159. doi:10.1039/C6TB02530G.

AB3-Loaded and Tumor-Targeted Unimolecular Micelles for Medullary Thyroid Cancer Treatment

Renata Jaskula–Sztul[a,1], **Guojun Chen**[b,c,1], **Ajitha Dammalapati**[e], **April Harrison**[e], **Weiping Tang**[f], **Shaoqin Gong**[b,c,d,*], and **Herbert Chen**[a,**]

[a]Department of Surgery, School of Medicine University of Alabama at Birmingham, Birmingham, AL 35233, USA

[b]Department of Materials Science and Engineering, University of Wisconsin–Madison, Madison, WI 53715, USA

[c]Wisconsin Institute for Discovery, University of Wisconsin–Madison, Madison, WI 53715, USA

[d]Department of Biomedical Engineering, University of Wisconsin–Madison, Madison, WI 53706, USA

[e]Department of Surgery, School of Medicine and Public Health, University of Wisconsin–Madison, Madison, WI 53706, USA

[f]School of Pharmacy, University of Wisconsin–Madison, Madison, WI 53706, USA

Abstract

Medullary thyroid cancer (MTC) is often resistant to standard therapies, emphasizing the need for the development of other treatments. A new histone deacetylase inhibitor, AB3, can effectively inhibit MTC cell proliferation *in vitro*. However, its poor aqueous solubility and stability, fast clearance, and lack of tumor targeting ability limit its *in vivo* application. Therefore, multifunctional unimolecular micelles were developed for targeted delivery of AB3 for MTC therapy. The unimolecular micelles exhibited a spherical core–shell structure, uniform size distribution, and excellent stability. AB3 was encapsulated into the hydrophobic core of the unimolecular micelles, thus significantly enhancing its aqueous solubility and stability. KE108, a somatostatin analog possessing high affinity to all five subtypes of SSTR, was used as an MTC-targeting ligand. *In vitro* cellular uptake analyses demonstrated that the KE108 exhibited superior targeting ability in MTC cells compared to octreotide, the first clinically used somatostatin analog. Moreover, the AB3-loaded and KE108-conjugated unimolecular micelles exhibited the best efficacy in suppressing MTC cell growth and tumor marker expression *in vitro*. Furthermore, AB3-loaded, KE108-conjugated micelles demonstrated the best anticancer efficacy *in vivo* without any apparent systemic toxicity, thereby offering a promising approach for targeted MTC therapy.

TOC image

Multifunctional unimolecular micelles conjugated with KE108, a superior MTC-targeting ligand, were developed for targeted delivery of AB3 to treat MTC.

*Corresponding author. shaoqingong@wisc.edu. **Corresponding author. herbchen@uab.edu.

[1]These authors contributed equally.

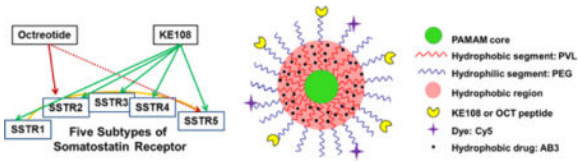

Keywords

Medullary thyroid cancer; somatostatin receptor; KE108; targeted drug delivery; HDAC inhibitor; unimolecular micelles

1. Introduction

Medullary thyroid cancer (MTC) is a neuroendocrine tumor that arises from the calcitonin-producing C-cells of the thyroid. While MTC accounts for only 5% of all thyroid cancers, it causes approximately 14% of all deaths from thyroid cancers[1, 2]. Surgery at a relatively early stage remains the only potential cure for MTC[3, 4]. Despite complete surgical resection, more than 50% of patients with MTC will have persistent or recurrent disease[5]. More importantly, MTC liver metastases are almost always small and widely distributed throughout the liver, precluding curative surgical resection[6]. Unfortunately, there are no effective treatments for patients with MTC liver metastases and/or widely metastatic diseases[7]. Thus, there is an urgent need for new treatment modalities for metastatic diseases.

Our previous studies showed that the inhibition of histone deacetylases (HDACs) triggered activation of Notch signaling and induced cell cycle arrest and apoptosis, leading to MTC cell growth suppression[7]. HDAC inhibitors have emerged as a new type of anticancer agent. Up to now, there have been three FDA-approved HDAC inhibitors, including SAHA[8], PXD-101[9], and natural product FK228[10]. AB3, a new synthetic HDAC inhibitor identified by Tang et al.[11], was easily prepared by condensing commercially available para-methoxybenzaldehyde with a known bifunctional reagent, which has a six methylene carbon tether between a hydrazide and a hydroxamic acid. We have demonstrated that AB3 can effectively inhibit MTC proliferation and suppress the expression of tumor markers, thereby making it a promising candidate as an anticancer drug for MTC treatment[7]. However, AB3, like most of the anticancer drugs, has poor aqueous solubility and stability, experiences fast *in vivo* clearance, and lacks *in vivo* tumor-targeting capabilities when administered systemically, thus limiting its application.

Drug nanocarriers have been wildly explored to overcome the limitations of conventional drugs, including poor solubility in aqueous media, inadequate stability, and lack of selectivity for tissues/cells[12–14]. Particularly, drug nanocarriers are attractive for targeted cancer therapy due to their passive (via the enhanced permeability and retention (EPR) effect) and active (via cell-specific ligand conjugation) tumor-targeting capabilities[13–15]. Among the various drug nanocarriers, polymer micelles, exhibiting a core–shell structure, have been extensively studied. Hydrophobic payloads can be readily encapsulated into the hydrophobic core of the micelles through hydrophobic interactions as well as hydrogen bonding, while the hydrophilic shell provides micelles with excellent aqueous

dispersibility[16–18]. Typically, polymer micelles are formed by the self-assembly of multiple linear amphiphilic block copolymers. However, one major concern with these conventional polymer micelles is their stability due to the dynamic nature of the self-assembly process. The *in vivo* stability of these self-assembled micelles can be affected by the concentration of the amphiphilic block copolymer molecules (critical micelle concentration), pH, ionic strength, temperature, or their interaction with serum proteins[19–21]. Premature rupture of these drug nanocarriers during circulation can cause a burst release of payloads into the bloodstream, which can cause potential systemic toxicity and surrender their tumor-targeting ability, thereby limiting their *in vivo* applications. Unimolecular micelles—formed by individual multi-arm star amphiphilic block copolymers—have been investigated to overcome this problem[22–27]. Because of their covalent nature and unique chemical structure, properly engineered unimolecular micelles can possess excellent *in vivo* stability. Moreover, due to their excellent chemical versatility, these unique unimolecular micelles have been successfully functionalized with different targeting ligands (e.g. small molecules, peptides, antibodies, and aptamers) and imaging probes (e.g., dyes, radioisotopes, etc.)[27–30].

The majority of MTCs overexpress five subtypes of somatostatin receptors (SSTR 1–5)[24, 31–33]. KE108 peptide is a somatostatin analog displaying strong binding affinities to all five subtypes of SSTRs. Our recent report demonstrated, for the first time, that KE108, a true pansomatostatin synthetic nonapeptide, can be used as an efficient SSTR-targeting ligand for targeted carcinoid cancer therapy[34]. In this study, we aimed to develop multifunctional unimolecular micelles for targeted MTC treatment (Figure 1 (A)). KE108 or octreotide (OCT) as an MTC-targeting ligand was conjugated to the unimolecular micelles. OCT peptide is the first somatostatin analog used in clinic[35]. However, it only displays a high binding affinity to SSTR2, and a moderate affinity to SSTR5, but has very little affinities to the other three SSTR subtypes (i.e., SSTR1, SSTR3, and SSTR4)[36–38]. Our studies demonstrate that, in comparison to OCT, KE108 was much more effective in enhancing the cellular uptake of micelles in MTC cells. AB3 was encapsulated into the hydrophobic core of the unimolecular micelles. AB3-loaded and KE108-conjugated unimolecular micelles were much more effective at suppressing MTC cell growth and tumor marker production. Moreover, *in vivo* studies demonstrated that the AB3-loaded and KE108-conjugated micelles exhibited the best antitumor efficacy, thus offering a promising approach for targeted MTC therapy.

2. METHODS

2.1 Synthesis of PAMAM–PVL–PEG–OCH_3/Cy5/KE108 and PAMAM–PVL–PEG–OCH_3/Cy5/OCT

PAMAM–PVL–PEG–OCH_3/Cy5/KE108 and PAMAM–PVL–OCH_3/Cy5/OCT polymers were synthesized following the scheme shown in Figure 1 (B). Detailed experimental procedures can be found in the Supplementary Materials. All of the intermediates and final polymer products were fully characterized by ^{1}H NMR (Figure S1 and S2 in the Supplementary Materials), Fourier transform infrared (FT–IR) spectroscopy (Figure S1), and gel permeation chromatographer (GPC, Table S1).

2.2 Preparation of AB3-Loaded Unimolecular Micelles

To prepare the AB3-loaded targeted (i.e., KE108-conjugated) unimolecular micelles, AB3 (5 mg) and PAMAM–PVL–PEG–OCH_3/KE108 (20 mg) were dissolved in acetonitrile (3 mL). Thereafter, DI water (9 mL) was added dropwise into the solution. The resulting mixture was stirred for 4 h at room temperature before acetonitrile was fully removed by rotary evaporation. The final AB3-loaded targeted unimolecular micelles were obtained after freeze-drying. The AB3-loaded non-targeted unimolecular micelles were prepared following a similar method using the PAMAM–PVL–PEG–OCH_3 polymer instead. The AB3 drug loading level, defined as the weight percentage of AB3 in the AB3-loaded unimolecular micelles, was measured by UV-vis spectroscopy at 293 nm.

2.3 *In Vitro* Release of AB3 from AB3-Loaded Unimolecular Micelles

The release profiles of AB3 from AB3-loaded micelles were studied in a glass apparatus at 37 °C in a release medium at pH 5.3 or 7.4[39]. Briefly, AB3-loaded unimolecular micelles (5 mg) dispersed in a medium (5 mL) were enclosed in a dialysis bag with a molecular weight cut-off of 2 kDa. The dialysis bag was immersed in 50 mL of the release medium and kept at 37 °C under a horizontal laboratory shaker at 100 rpm (Thermo Scientific MaxQ Shaker, USA). At specific time points, 3 mL of release media were collected and replaced by the same volume of fresh media. The amount of released AB3 was analyzed by a UV–Vis–NIR spectrophotometer at 293 nm.

2.4 Quantitative Real-Time PCR of SSTR 1–5 Receptors in TT Cells

The mRNA expression levels of SSTRs in TT cells were measured by qRT–PCR. RNA was isolated and transcribed into cDNA following a protocol published previously[40]. A qRT–PCR reaction was performed using a CFX Thermal Cycler and SsoFast EvaGreen labeling system (Bio-Rad) at conditions described earlier[41] on three biological replicates. The SSTR 1–5 primer sequences were as follows: SSTR1 forward, 5′-ATGGTGGCCCTCAAGGCCGG-3′ and reverse, 5′-CGCGGTGGCGTAATAGTCAA-3′; SSTR2 forward, 5′-CCAACACCTCAAACCAGAC-3′ and reverse, 5′-CATAGCCAAGAAAGGCAGAC-3′; SSTR3 forward, 5′-TCATCTGCCTCTGCTACCTG-3′ and reverse, 5′-GAGCCCAAAGAAGGCAGGCT-3′; SSTR4 forward, 5′-ATCTTCGCAGACACCAGACC-3′ and reverse, 5′-ATCAAGGCTGGTCACGACGA-3′; SSTR5 forward, 5′-CCGTCTTCATCATCTAACACGG-3′ and reverse, 5′-GGCCAGGTTGACGATGTTGA-3′. The s27 primer sequences were as follows: forward, 5′-TCTTTAGCCATGCACAAACG-3′ and reverse, 5′-TTTCAGTGCTGCTTCCTCCT-3′. The mRNA expression levels of the SSTRs in MZ–CRC–1 cells were measured following a similar procedure[34]. Both TT and MZ–CRC–1 are human MTC cell lines.

The cycle numbers obtained at the log–linear phase of the reactions for target genes were normalized to housekeeping gene *s27* from the same sample measured concurrently. Finally, the expression ratios were calculated using the comparative cycle threshold (ΔC_t) method and presented as the average ± standard error of the mean (SEM).

2.5 Cellular Uptake Analyses

The cellular uptake behaviors of the micelles in a human MTC cell line (i.e., TT) were analyzed using both flow cytometry and confocal laser scanning microscopy (CLSM). Multi-arm star amphiphilic block copolymers PAMAM–PVL–PEG–OCH_3/Cy5/KE108, PAMAM–PVL–PEG–OCH_3/Cy5/OCT, and PAMAM–PVL–PEG–OCH_3/Cy5 were dissolved in the cell culture medium directly to form the KE108-conjugated, OCT-conjugated, and non-targeted micelles, respectively. For flow cytometry analyses, cells were seeded in 6-well plates (3×10^5 cells/mL) and incubated overnight. Cells were treated with KE108-conjugated, OCT-conjugated, or non-targeted micelles (100 μg/mL). The culture medium was used as a blank control. After 2 h of incubation, the cells were washed with PBS and lifted using a non-enzymatic cell dissociation solution. The cellular uptake of the micelles based on Cy5 intensity was analyzed using a FACS Calibur four-color analysis cytometer (Becton Dickinson, San Jose, CA) and FlowJo analysis software (Tree Star, Inc., Ashland, OR). A minimal of 1×10^5 cells were analyzed for each sample. The cellular uptake of the micelles in WI-38 (pulmonary fibroblasts), a cell line that does not overexpress SSTRs, was studied following similar procedures using flow cytometry and was used as a negative control. For the CLSM studies, cells were seeded (1×10^5 cells/mL) onto 96-well high-optical-quality plates and incubated overnight. Cells were treated with either KE108-conjugated (i.e., targeted) or non-targeted micelles (100 μg/mL). After 2 h of incubation, the cells were washed with PBS, fixed with 1.5% formaldehyde for 15 min, and washed with DI water. Then the cells on the optical plate were mounted with Prolong Gold anti-fade reagent with DAPI (Life Technologies, Carlsbad, CA) and the images were taken under a Nikon A1R–Si high-speed spectral laser scanning confocal inverted microscope (Nikon, Melville, NY) with NIS-Elements BR Software.

2.6 Cell Proliferation Assays

The cytotoxicity of free AB3 and AB3-loaded micelles with or without KE108-targeting ligands on two human MTC cell lines (i.e., TT and MZ–CRC–1) was assessed using MTT assays. Cells were plated on 96-well plates and incubated overnight. Cells were treated with pure medium, free AB3, AB3-loaded targeted and non-targeted micelles, and empty targeted and non-targeted micelles (AB3-free micelles). The equivalent AB3 concentration for all AB3-loaded micelles was 3 μM[42]. The cells were then incubated for 24, 48, and 96 h, and the MTT assay was performed at each time point using a standard protocol[26]. The plates were then measured at 570 nm using a spectrophotometer (Quant, Bio-Tek Instruments, Winooski, VT). The percent of cell viability relative to the control (pure medium) was calculated.

2.7 Tumor Marker Expression Assays

MTC marker expressions, including achaete–scute complex-like 1 (ASCL-1) and chromogranin A (CgA), were assessed using Western blot analyses. Cells were seeded in 100 mm culture plates and incubated overnight. Cells were then treated with pure medium, free AB3 (3 μM), or AB3-loaded, KE108-conjugated targeted and non-targeted micelles. The equivalent AB3 concentration for all AB3-loaded micelles was 3 μM. After incubation for 48 h, proteins were harvested according to a previously described protocol[31]. Protein

concentrations were determined by a bicinchoninic acid assay (Thermo Scientific, Waltham, MA). The protein lysates (20 μg) were denatured and resolved on 10% SDS–PAGE gels. Protein bands in the gel were then transferred to a nitrocellulose membrane and incubated with the appropriate primary antibody with dilutions as follows: 1:2000 for ASCL-1, 1:1000 for CgA, and 1:1000 for β-actin. Membranes were incubated overnight at 4 °C and then washed with buffer (1×PBS, 0.05% Tween 20). Horseradish peroxidase-conjugated goat, anti-rabbit, or anti-mouse secondary antibodies were used for secondary incubation. Proteins were then visualized with chemiluminescent substrates Immunstar (CgA and β-actin) or Femto (ASCL-1). The quantitative analyses of the protein expression of ASCL1 and CgA were done using ImageJ bundled with Java 1.8.0_77 (http://imagej.nih.gov/ij/).

2.8 *In Vivo* Anticancer Study

Four-week-old male athymic nude mice were obtained from Charles River (Wilmington, Maryland, USA). A subcutaneous MTC tumor xenograft model was established by subcutaneously implanting 1×10^7 TT cells in 200 μL of Hanks balanced salt solution (Mediatech, Inc, Manassas, Virginia, USA) into the left flank of each mouse. Ten days after inoculation, TT-tumor-bearing mice were randomly divided into six treatment groups (6 mice/per group). The six groups of mice were treated with saline (control), free AB3, AB3-loaded non-targeted micelles, AB3-loaded, KE108-conjugated targeted micelles, empty non-targeted micelles, and empty KE108-conjugated targeted micelles at the equivalent AB3 dose of 20 mg/kg BW. Each treatment group received five intravenous injections every five days. Tumor volumes were measured by a caliper and then calculated by the modified ellipsoidal formula: Tumor volume = (length × width^2) / 2. At the end of the experiment, mice were sacrificed and postmortem examination of the lungs, liver, heart, and spleen were performed to confirm that there was no evidence of metastases or tumor growth outside of the inoculation site. All major organs, including the liver, brain, heart, and leg muscles, of the mice treated with AB3-loaded targeted micelles were collected and hematoxylin and eosin (H&E)-stained sections were prepared for pathological assessment. All experimental procedures were carried out in compliance with our animal care protocol (M01474-0-01-09), which was approved by the Animal Care and Use Committee of the University of Wisconsin-Madison.

2.9 Statistical Analysis

Weights and volumes were compared between groups using an analysis of variance (ANOVA) with pair-wise comparisons performed using Fisher's protected least significant difference tests. Data were log-transformed prior to analyses to better meet the assumptions of the ANOVA. P-values less than 0.05 were considered to be statistically significant.

3. RESULTS

The synthesis of multi-arm star amphiphilic block copolymer PAMAM–PVL–PEG–OCH_3/Cy5/KE108 or PAMAM–PVL–PEG–OCH_3/Cy5/OCT was carried out following Figure 1 (B). First, PAMAM–PVL–OH was prepared by the ring-opening polymerization of valerolactone (VL) using PAMAM–OH (G4, 64 –OH terminal groups) as a macroinitiator. The terminal –OH groups of PAMAM–PVL–OH were then converted into –COOH by

reacting with succinic anhydride to form PAMAM–PVL–COOH. Thereafter, two types of PEG (namely, OH–PEG–OCH_3 and OH–PEG–NHS) were conjugated onto the PAMAM–PVL–COOH via an esterification reaction. The NHS functional groups were used subsequently to conjugate the targeting ligand (KE108 or OCT) and Cy5 dye. All of the intermediates and final products were fully characterized by ^{1}H NMR, FT–IR and GPC analyses as shown in Supplementary Materials.

The resulting multi-arm star amphiphilic block copolymers formed stable unimolecular micelles in an aqueous solution. The hydrophobic core of the micelles allowed for the encapsulation of the hydrophobic drug AB3 through hydrophobic interactions and hydrogen bonding, thereby enhancing the water solubility and stability of AB3. Peptides KE108 or OCT on the surface of the unimolecular micelles provided the micelles with specific SSTR targeting abilities. The effects of KE108 and OCT targeting ligands on the cellular uptake of the micelles were studied and will be discussed later. The Cy5 dye conjugated onto the micelles allowed for the visualization of the micelles. The average hydrodynamic size of the unimolecular micelles measured by dynamic light scattering (DLS, Figure S3 (A)) was 58 nm (PDI = 0.114). The unimolecular micelles showed a spherical morphology with a clear core–shell structure under transmission electron microscopy (TEM, Figure S3 (B)). The drug-loading level and drug-loading efficiency of AB3-loaded unimolecular micelles were 15.1% and 76.6%, respectively.

The *in vitro* drug release profiles are shown in Figure 2. A clear pH-dependent drug release behavior was observed. At pH = 7.4, only 15% of AB3 was released after 5 days. In contrast, at pH = 5.3, a relatively rapid drug release rate was observed with 59% of AB3 being released after 5 days. The pH-dependent drug release behavior could be possibly due to the fact that the hydrophobic core of the micelle, within which AB3 was encapsulated, was made of PVL, a member of the polyester family, which can be hydrolyzed faster under acidic conditions, thereby leading to a faster drug release[43–46]. Swelling of the PAMAM in an acidic condition due to the protonation of the 62 tertiary amine groups in an acidic condition could be another possible reason[47–49].

The efficacy of KE108 as an SSTR-targeting ligand for MTC cells was evaluated first *in vitro*. As shown in Figure 3 (A), two MTC cell lines (TT and MZ-CRC-1) have high expression of all five SSTRs except for SSTR4. To test whether KE108 has a superior targeting compared to OCT, TT cells were treated with either non-targeted (without any targeting ligand) unimolecular micelles or unimolecular micelles conjugated with either KE108 or OCT. Based on the fluorescent intensity of the Cy5 dye conjugated on the micelles, the cellular uptake of the micelles was measured by flow cytometry. As shown in Figure 3 (B), OCT—which has a high affinity for SSTR2, a moderate affinity for SSTR5, and very little affinity to SSTR1, SSTR3, and SSTR4—increased the cellular uptake of the micelles 4-fold compared with non-targeted micelles. The KE108 peptide, on the other hand, has a high affinity for all 5 subtypes of SSTRs (SSTR 1–5) and thus was expected to display much better targeting efficacy than OCT. Indeed, the intracellular uptake of the KE108-conjugated micelles was 50 and 15 times higher than that of the non-targeted micelles and OCT-conjugated micelles, respectively. To further demonstrate the specific SSTR targeting ability of KE108, the cellular uptake behavior of the unimolecular micelles in a WI-38 cell

line (pulmonary fibroblasts), that does not overexpress SSTRs, was also studied and no differences were observed in the level of cellular uptake between the KE108-conjugated, OCT-conjugated, or non-targeted micelles (Figure 3 (C)). These findings indicate that MTC cells overexpressing SSTRs on their surface exhibited an increased intracellular uptake of KE108-conjugated micelles through the SSTR-mediated endocytosis process. Furthermore, KE108 peptides exhibited a much more superior SSTR-targeting ability than OCT due to its high affinity for all five SSTR subtypes (SSTR 1–5).

The targeting ability of KE108 was further confirmed by CLSM analyses (Figure 4). As expected, targeted (KE108-conjugated) unimolecular micelles exhibited significantly higher cellular uptake than non-targeted micelles, manifested by much stronger red Cy5 fluorescence. Moreover, both non-targeted and targeted micelles accumulated preferentially in the cytoplasm of the cells because nanoparticles were taken up via an endocytosis process[23]. Overall, the greater cellular uptake of the targeted micelles compared to the non-targeted ones revealed that the KE108-targeting ligand was effective at promoting SSTR-mediated endocytosis. In contrast, non-targeted micelles were taken up through non-specific endocytosis.

To further demonstrate the superior targeting ability of KE108, the anti-proliferative efficacies of AB3-loaded micelles were evaluated in MTC cells (i.e., TT and MZ–CRC–1). As shown in Figure 5 (A) and (B), at each time point (24, 48, or 96 h), AB3-loaded targeted (i.e., KE108-conjugated) micelles (i.e., AB3-T) exhibited the best efficacy of suppressing proliferation in both TT and MZ-CRC-1 cells in comparison with other treatment groups. The enhanced cytotoxicity of AB3-T over non-targeted ones (i.e., AB3-NT) was attributed to their enhanced cellular uptake as discussed above. Moreover, neither the empty non-targeted (i.e., Empty NT) micelles nor targeted (i.e., Empty T) ones exhibited any apparent cytotoxicity. Notably, it was also observed that cells treated with AB3-T were more sensitive than free AB3. To further investigate the effect of KE108 conjugation on the anticancer efficacy of AB3-loaded targeted micelles, Western blot analyses on MTC marker expression in MTC cells were carried out. ASCL-1 and CgA are well established MTC markers, and high levels of ASCL-1 and CgA are linked to the poor prognosis of MTC[50, 51]. As shown in Figure 5 (C) and (D), the AB3-T were much more effective in reducing the expression of both ASCL-1 and CgA than AB3-NT as well as free AB3, which is in good agreement with the MTT results. The quantitative analyses of Western blot data are shown in the Figure S4.

The antitumor study of the AB3-loaded micelles *in vivo* was then performed. TT-tumor-bearing mice were intravenously treated with saline (control), pure AB3, empty non-targeted micelles (Empty NT), empty targeted (i.e., KE108-conjugated) micelles (Empty T), AB3-loaded non-targeted micelles (AB3-NT), or AB3-loaded targeted micelles (AB3-T) at an equivalent AB3 dosage of 20 mg/kg BW every five days for a total of five treatments. As shown in Figure 6 (A), neither Empty NT nor Empty T induced any antitumor effect, while all drug treatment groups significantly decreased the tumor burden as compared to the saline control group. However, AB3-T induced the highest antitumor efficacy among all treatment groups. No noticeable changes in body weight or survival were observed in the AB3-NT or AB3-T groups. In contrast, while free AB3 also exhibited inhibition of tumor growth when compared to the control, its severe toxicity in mice was demonstrated by decreased survival

(3 out of the 6 mice died during the experiment). Pathological assessment of H&E–stained sections of different organs (i.e., brain, heart, liver and leg muscles) of mice treated with AB-T micelles (Figure 6 (B)) did not indicate any signs of acute or chronic inflammation, or apoptotic or necrotic regions, suggesting that the AB3-loaded targeted unimolecular micelle delivery system was safe for organs other than the NE cancerous tissues, and that the potential off-target uptake of micelles by normal tissues did not cause any detectable damage. These findings may support the development of AB3-loaded, KE108-conjugated tumor-targeting unimolecular micelles in the treatment and palliation of patients with MTC cancers. This approach can significantly enhance the therapeutic outcome of cancer therapy while minimizing undesirable side-effects.

4. DISCUSSION

MTC, derived from the parafollicular cells (C-cells) of the thyroid, is an aggressive subtype of thyroid cancers[1, 2]. Like most thyroid cancers, surgical resection is the predominant treatment modality and can be curative in selected patients. However, unlike well-differentiated thyroid cancers which can be treated with surgery and/or radioactive iodine even when metastases develop, patients with MTC metastases have limited options. Hence, it is of great importance to developing other effective treatment modalities. We have recently reported that AB3, a new HDAC inhibitor, can effectively inhibit MTC proliferation and suppress the expression of tumor markers[7]. In order to further increase its therapeutic indexes and minimize its off-target toxicities, in this study, we have successfully developed a multifunctional unimolecular micelle for targeted delivery of AB3 for MTC treatment. Unimolecular micelle was formed by individual multi-arm star amphiphilic block copolymer PAMAM–PVL–PEG–OCH_3/KE108/Cy5. All of the components of the unimolecular micelles were covalently linked, thereby conferring outstanding stability. Moreover, the average hydrodynamic size of the micelles was 58 nm, which is desirable for tumor-targeted drug delivery[52]. AB3 was physically loaded into the hydrophobic core of the unimolecular micelles via hydrophobic interaction as well as hydrogen bonding. The *in vitro* drug release study showed that AB3 was released in a pH-dependent manner. This pH-dependent release behavior is of particular interest for drug delivery systems for cancer therapies. It is expected that AB3 is sufficiently stable in micelles with minimal drug leakage during blood circulation. After the AB3-loaded micelles are taken up by cancer cells through endocytosis, where acidic endosomes or lysosomes are involved, AB3 will be released relatively quickly to effectively kill the cancer cells.

Somatostatin analogs, KE108 and OCT, were used as the targeting ligand. Through quantitative flow cytometry analyses, we demonstrated that both KE108-conjugated and OCT-conjugated micelles were taken up to a greater extent than non-targeted micelles in MTC cells. Meanwhile, the cellular uptake of the KE108-conjugated micelles exhibited superior targeting ability compared to OCT-conjugated micelles, which is due to the fact that KE108 peptide possesses high affinity for all five subtypes of somatostatin receptors (SSTR 1–5), while OCT, the clinically used somatostatin analog, only displays high affinity to SSTR2. It is worth mentioning that other than MTCs, these KE108-conjugated micelles can also be potentially used as targeted drug nanocarriers for several other types of cancers that overexpress SSTRs, including melanomas[53] and breast cancers[54].

The KE108-functionalized AB3-loaded unimolecular micelles were able to suppress cell growth and tumor marker expression in MTC cells to a significantly greater extent compared to non-targeted ones, further demonstrating the targeting ability of KE108. It is noted that the KE108 functionalized AB3-loaded unimolecular micelles also exhibited better anticancer effect than free AB3 *in vitro*. These differences may be attributable to two possible reasons. First, it may be due to the different mechanisms of cellular uptake for free drug versus drug encapsulated in targeted micelles. The cellular uptake of free AB3 occurs through a passive diffusion mechanism and the drug may be expelled out through the P-glycoprotein (P-gp) pump[55], while AB3-T were taken up by receptor-mediated endocytosis, which may overcome the P-gp pumping action[56]. Second, it might be due to the poor solubility and stability of free AB3. The stability and solubility of AB3 loaded inside of the targeted micelles can be greatly enhanced. In addition to highlighting the ability of KE108-conjugated micelles to effectively target and deliver AF to MTC cells *in vitro*, we studied the *in vivo* anti-tumor efficacy. AB3-loaded targeted micelles demonstrated a much higher anti-tumor effect statistically compared to other treatments groups. H&E analyses on the major organs did not show any indication of inflammation, or apoptotic or necrotic regions. However, the pure AB3 treatment group showed a low survival rate (3 out of the 6 mice died).

Currently, the majority of drug discovery and development efforts for MTCs have been limited to somatostatin analogs and repurposing various existing anticancer drugs. Both approaches have significant shortcomings. First, somatostatin analogs lack adequate anti-proliferative efficacy against MTCs and patients develop resistance to the therapy over time. Second, systemic non-targeted delivery of chemotherapeutics can lead to profound side effects. Our findings address these major issues by demonstrating that (1) SSTRs can serve as targets for patients with MTCs, (2) KE108 peptide can be used as a superior targeting ligand for SSTRs in comparison with other common somatostatin analogs, such as OCT, and (3) unimolecular micelles conjugated with KE108 can serve as drug delivery vehicles for any hydrophobic anticancer drugs including therapeutic HDACis such as AB3, which will reduce systemic side-effects.

5. CONCLUSIONS

The multifunctional unimolecular micelles made of multi-arm star amphiphilic block copolymer PAMAM–PVL–PEG–OCH_3/KE108/Cy5 were developed for targeted MTC therapy. KE108 peptide, displaying high affinity to all five subtypes of SSTRs (SSTR 1–5), was employed as a novel targeting moiety for MTCs overexpressing SSTRs. The cellular uptake of the targeted unimolecular micelles in the MTC cells was dramatically enhanced compared to that of either OCT-conjugated ones or non-targeted ones. Moreover, AB3-loaded and KE108-conjugated unimolecular micelles were much more effective at suppressing MTC cell growth and hormone production than other types of micelles or free AB3. Finally, *in vivo* studies demonstrated that the AB3-loaded and KE108-conjugated micelles exhibited the best antitumor efficacy. Thus, these AB3-loaded and KE108-conjugated micelles offer a promising approach for targeted MTC therapy.

Supplementary Material

Refer to Web version on PubMed Central for supplementary material.

Acknowledgments

This project was financially supported by grants from the NIH (R01 CA121115 to H. Chen, 1K25CA166178 and R21CA196653 to S. Gong), the Aly Wolff Memorial Foundation (S. Gong and H. Chen), the American Cancer Society (MEN2 Thyroid Cancer Professorship 120319–RPM–11–080–01–TBG to H. Chen and Research Scholar Award RSGM TBE–121413 to H. Chen), the Caring for Carcinoids Foundation, and the AACR. The authors would like to thank Dr. Ricardo Lloyd for the pathological assessment of the mice tissues and Dr. Glen Leverson for the statistical analysis.

References

1. Schlumberger M, Carlomagno F, Baudin E, Bidart JM, Santoro M. Nature clinical practice Endocrinology & metabolism. 2008; 4:22–32.
2. Papotti M, Kumar U, Volante M, Pecchioni C, Patel YC. Chinical Endocrinology. 2001; 54:641–649.
3. Greenblatt DY, Vaccaro AM, Jaskula-Sztul R, Ning L, Haymart M, Kunnimalaiyaan M, Chen H. The oncologist. 2007; 12:942–951. [PubMed: 17766653]
4. Sippel RS, Kunnimalaiyaan M, Chen H. The oncologist. 2008; 13:539–547. [PubMed: 18515739]
5. Hahm HR, Lee MS, Min YK, Lee MK, Kim KW, Nam SJ, Yang JH, Chung JH. Thyroid. 2004; 11:73–80.
6. Chen H, Robert JR, Ball DW, Eisele DW, Baylin SB, Udelsman R, Bulkley G. Ann Surg. 1998; 227:887–895. [PubMed: 9637552]
7. Jaskula-Sztul R, Eide J, Tesfazghi S, Dammalapati A, Harrison AD, Yu XM, Scheinebeck C, Winston-McPherson G, Kupcho KR, Robers MB, Hundal AK, Tang W, Chen H. Molecular cancer therapeutics. 2015; 14:499–512. [PubMed: 25512616]
8. Duvic M, Talpur R, Ni X, Zhang C, Hazarika P, Kelly C, Chiao JH, Reilly JF, Ricker JL, Richon VM, Frankel SR. Blood. 2007; 109:31–39. [PubMed: 16960145]
9. Lee HZ, Kwitkowski VE, Del Valle PL, Ricci MS, Saber H, Habtemariam BA, Bullock J, Bloomquist E, Li Shen Y, Chen XH, Brown J, Mehrotra N, Dorff S, Charlab R, Kane RC, Kaminskas E, Justice R, Farrell AT, Pazdur R. Clinical cancer research : an official journal of the American Association for Cancer Research. 2015; 21:2666–2670. [PubMed: 25802282]
10. VanderMolen KM, McCulloch W, Pearce CJ, Oberlies NH. The Journal of antibiotics. 2011; 64:525–531. [PubMed: 21587264]
11. Tang W, Luo T, Greenberg EF, Bradner JE, Schreiber SL. Bioorganic & medicinal chemistry letters. 2011; 21:2601–2605. [PubMed: 21334896]
12. Allen TM, Cullis PR. Science. 2004; 303:1818–1822. [PubMed: 15031496]
13. Shi J, Votruba AR, Farokhzad OC, Langer R. Nano Lett. 2010; 10:3223–3230. [PubMed: 20726522]
14. Pan JMKD, Hong S, Farokhzad OC, Margalit R, Langer R. Nature Nanotechnology. 2007; 2:751–760.
15. Wang AZ, Langer R, Farokhzad OC. Annual review of medicine. 2012; 63:185–198.
16. Torchilin VP. Nature reviews Drug discovery. 2005; 4:145–160. [PubMed: 15688077]
17. Torchilin VP. Pharmaceutical research. 2007; 24:1–16. [PubMed: 17109211]
18. Kedar U, Phutane P, Shidhaye S, Kadam V. Nanomedicine : nanotechnology, biology, and medicine. 2010; 6:714–729.
19. Heise A, Hedrick JL, Frank CW, Miller RD. JACS. 1999; 121:8647–8648.
20. Lawrence MJ. Chemical Society Reviews. 1994; 23:417–424.
21. Kim S, Shi Y, Kim J, Park K, Cheng J. Expert Opin Drug Deliv. 2010; 7:49–62. [PubMed: 20017660]

22. Prabaharan M, Grailer JJ, Pilla S, Steeber DA, Gong S. Biomaterials. 2009; 30:3009–3019. [PubMed: 19250665]
23. Prabaharan M, Grailer JJ, Pilla S, Steeber DA, Gong SQ. Biomaterials. 2009; 30:5757–5766. [PubMed: 19643472]
24. Xu W, Burke JF, Pilla S, Chen H, Jaskula-Sztul R, Gong S. Nanoscale. 2013; 5:9924–9933. [PubMed: 23986296]
25. Guo J, Hong H, Chen G, Shi S, Nayak TR, Theuer CP, Barnhart TE, Cai W, Gong S. ACS applied materials & interfaces. 2014; 6:21769–21779. [PubMed: 24628452]
26. Chen G, Wang L, Cordie T, Vokoun C, Eliceiri KW, Gong S. Biomaterials. 2015; 47:41–50. [PubMed: 25682159]
27. Xiao Y, Hong H, Javadi A, Engle JW, Xu W, Yang Y, Zhang Y, Barnhart TE, Cai W, Gong S. Biomaterials. 2012; 33:3071–3082. [PubMed: 22281424]
28. Guo J, Hong H, Chen G, Shi S, Zheng Q, Zhang Y, Theuer CP, Barnhart TE, Cai W, Gong S. Biomaterials. 2013; 34:8323–8332. [PubMed: 23932288]
29. Xu W, Siddiqui IA, Nihal M, Pilla S, Rosenthal K, Mukhtar H, Gong S. Biomaterials. 2013; 34:5244–5253. [PubMed: 23582862]
30. Jaskula-Sztul R, Xu W, Chen G, Harrison A, Dammalapati A, Nair R, Cheng Y, Gong S, Chen H. Biomaterials. 2016; 91:1–10. [PubMed: 26994874]
31. Xiao Y, Jaskula-Sztul R, Javadi A, Xu W, Eide J, Dammalapati A, Kunnimalaiyaan M, Chen H, Gong S. Nanoscale. 2012; 4:7185–7193. [PubMed: 23070403]
32. Sun LC, Coy DH. Current Drug Delivery. 2011; 8:2–10. [PubMed: 21034425]
33. Pinchot SN, Holen K, Sippel RS, Chen H. The oncologist. 2008; 13:1255–1269. [PubMed: 19091780]
34. Chen G, Jaskula-Sztul R, Harrison A, Dammalapati A, Xu W, Cheng Y, Chen H, Gong S. Biomaterials. 2016; 97:22–33. [PubMed: 27156249]
35. Lamberts SW, Van der Lely AJ, de Herder WW, Hofland LJ. New England Journal of Medicine. 1996; 334:246–254. [PubMed: 8532003]
36. Zou Y, Xiao X, Li Y, Zhou T. Oncology Reports. 2009; 21:379–386. [PubMed: 19148511]
37. Jiang H, Deng XF, Duan CM, Chen C, Xiang JL, Lu Y, Ma QF. Lymphology. 2011; 44:21–28. [PubMed: 21667819]
38. Shimon L, Taylor JE, Dong JZ, Bitonte RA, S K, Morgan B, Coy DH, Culler MD, Melmed S. J Clin Invest. 1997; 99:789–798. [PubMed: 9045884]
39. Bao Y, Yin M, Hu X, Zhuang X, Sun Y, Guo Y, Tan S, Zhang Z. Journal of Controlled Release. 2016; 235:182–194. [PubMed: 27264552]
40. Wyche TP, Dammalapati A, Cho H, Harrison AD, Kwon GS, Chen H, Bugni TS, Jaskula-Sztul R. Cancer gene therapy. 2014; 21:518–525. [PubMed: 25412645]
41. Jaskula-Sztul R, Pisarnturakit P, Landowski M, Chen H, Kunnimalaiyaan M. The Journal of surgical research. 2011; 171:23–27. [PubMed: 21571316]
42. Jaskula-Sztul R, Eide J, Tesfazghi S, Dammalapati A, Harrison AD, Yu X-M, Scheinebeck C, Winston-McPherson G, Kupcho KR, Robers MB. Molecular cancer therapeutics. 2015; 14:499–512. [PubMed: 25512616]
43. Shuai X, Ai H, Nasongkla N, Kim S, Gao J. Journal of Controlled Release. 2004; 98:415–426. [PubMed: 15312997]
44. Abulateefeh SR, Spain SG, Thurecht KJ, Aylott JW, Chan WC, Garnett MC, Alexander C. Biomaterials Science. 2013; 1:434–442.
45. Li D, Ding JX, Tang ZH, Sun H, Zhuang XL, Xu JZ, Chen XS. International journal of nanomedicine. 2012; 7:2687. [PubMed: 22701317]
46. Arya N, Katti DS. International journal of nanomedicine. 2015; 10:2997. [PubMed: 25945047]
47. van Dongen MA, Orr BG, Banaszak Holl MM. The Journal of Physical Chemistry B. 2014; 118:7195–7202. [PubMed: 24901764]
48. Kleinman MH, Flory JH, Tomalia DA, Turro NJ. The Journal of Physical Chemistry B. 2000; 104:11472–11479.

49. Maiti PK, Cagin T, Lin ST, Goddard WA. Macromolecules. 2005; 38:979–991.
50. Oberg K, Janson ET, Eriksson B. Ital J Gastroenterol Hepatol. 1999; 31:S160–S162. [PubMed: 10604122]
51. Chen H, Udelsman R, Zeiger MA, Ball DW. Oncol Rep. 1997; 4:775–778. [PubMed: 21590138]
52. Byrne JD, Betancourt T, Brannon-Peppas L. Advanced drug delivery reviews. 2008; 60:1615–1626. [PubMed: 18840489]
53. Martinez-Alonso M, Llecha N, Mayorga M, Sorolla A, Dolcet X, Sanmartin V, Abal L, Casanova J, Bardad M, Yeramian AE, Puig RS, Vilella R, Matias-Guiu X, Marti R. J Int Med Res. 2009; 37:1813–1822. [PubMed: 20146879]
54. Huo M, Zou A, Yao C, Zhang Y, Zhou J, Wang J, Zhu Q, Li J, Zhang Q. Biomaterials. 2012; 33:6393–6407. [PubMed: 22704599]
55. Liang P, Zhao D, Wang CQ, Zong JY, Zhuo RX, Cheng SX. Colloids and surfaces B, Biointerfaces. 2013; 102:783–788. [PubMed: 23104038]
56. Miller DW, Batrakova EV, Waltner TO, Alakhov VY, Kabanov AV. Bioconjugate Chemistry. 1997; 8:649–657. [PubMed: 9327127]

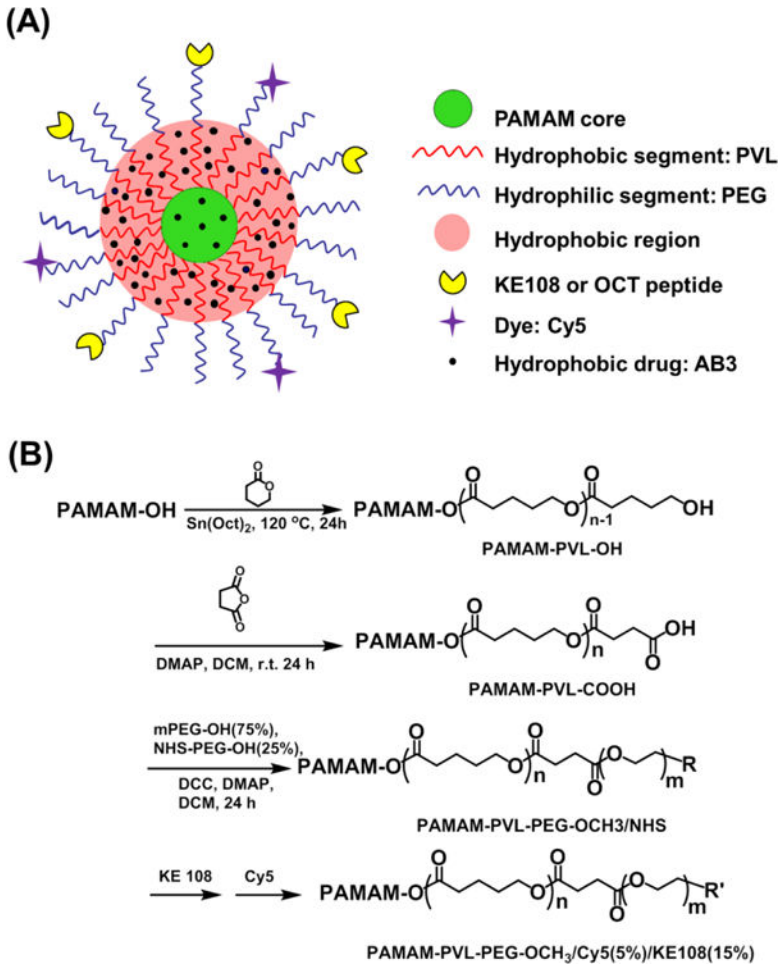

Figure 1.

(A) A schematic illustration of a multifunctional unimolecular micelle formed by multi-arm star amphiphilic block copolymer PAMAM–PVL–PEG–OCH_3/ Cy5/KE108 for targeted delivery of AB3 for MTC treatment. (B) A synthetic scheme of the multi-arm star amphiphilic block copolymers PAMAM–PVL–PEG–OCH_3/Cy5/KE108 or PAMAM–PVL–PEG–OCH_3/Cy5/OCT.

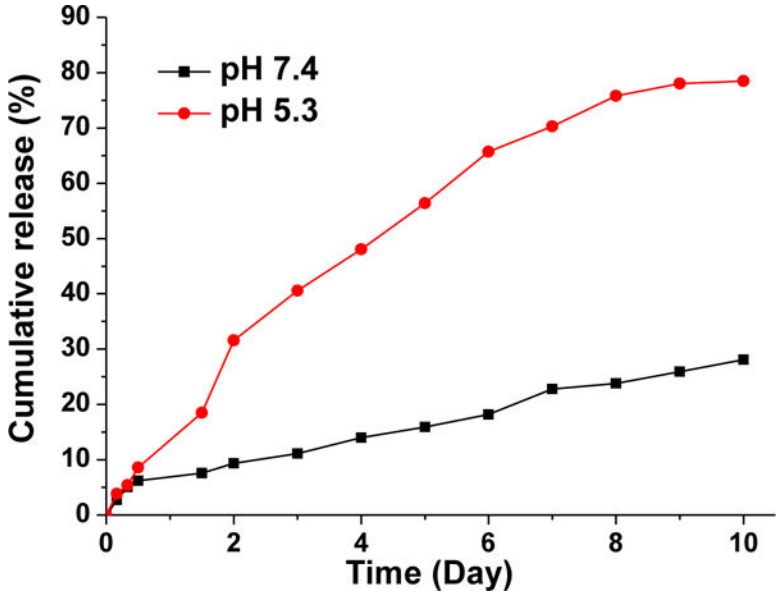

Figure 2.
In vitro release of AB3 from AB3-loaded unimolecular micelles.

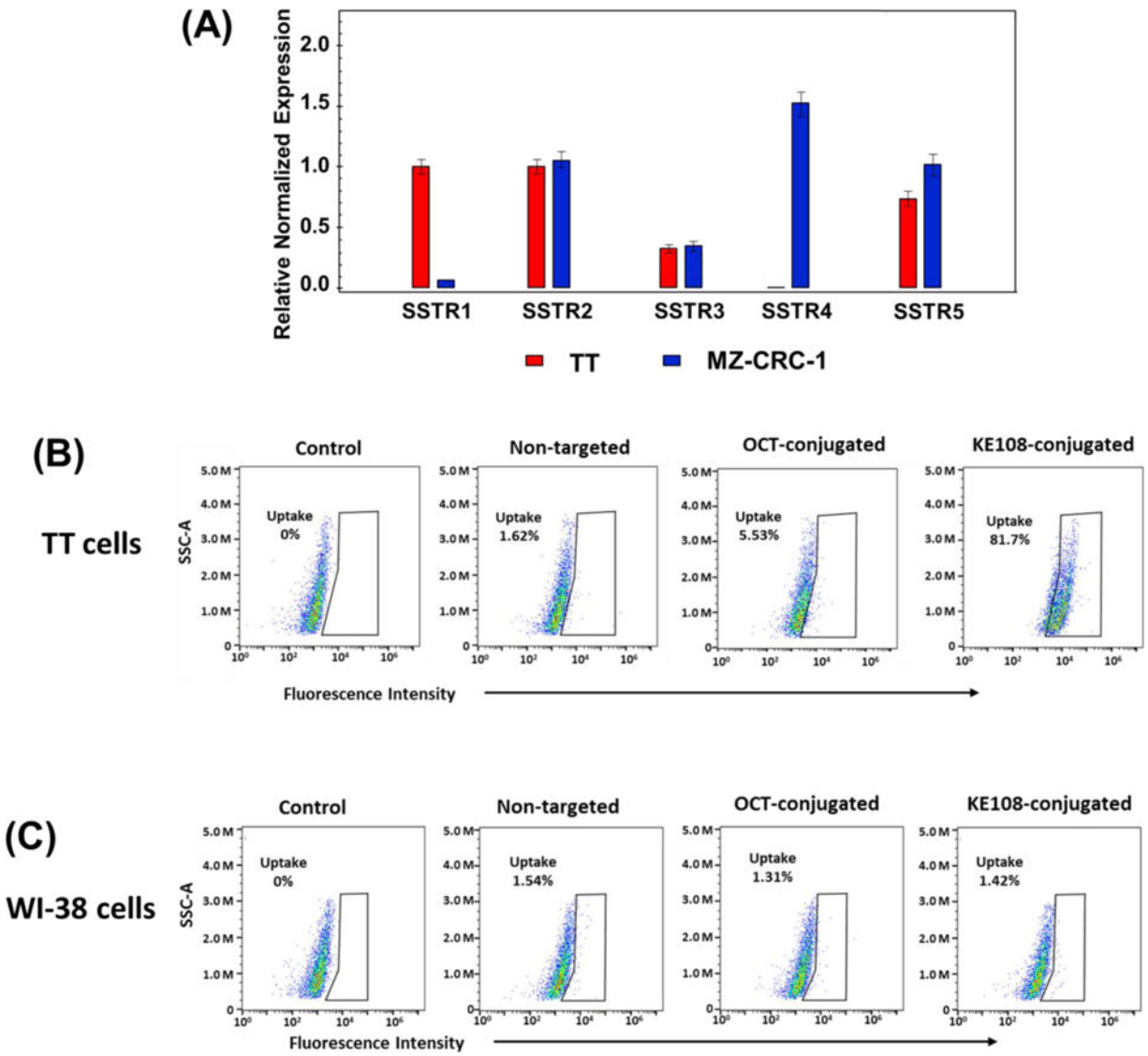

Figure 3.

(A) The expression levels of the five subtypes of SSTR in TT and MZ–CRC–1 cells. Flow cytometry analysis of the (B) TT and (C) WI-38 cells treated with pure medium (control), non-targeted, OCT-conjugated or KE108-conjugated unimolecular micelles (100 μg/mL) for 2 h at 37 °C.

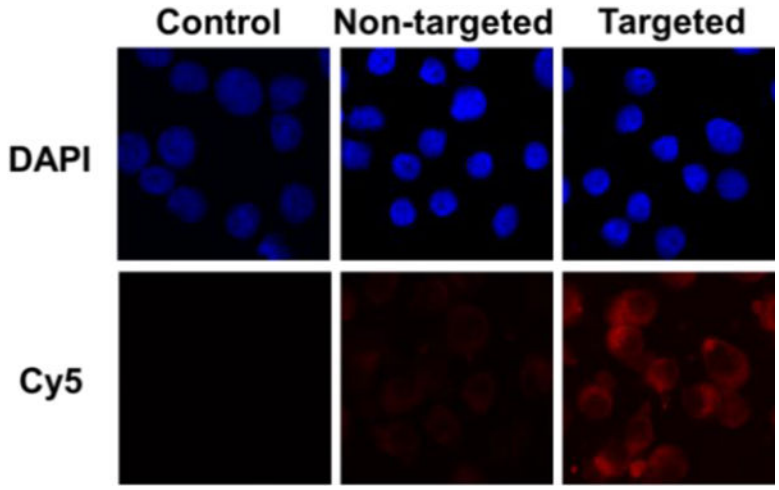

Figure 4.

CLSM images of TT cells treated with pure medium (control), or non-targeted or targeted (KE108-conjugated) unimolecular micelles (100 μg/mL) for 2 h at 37 °C.

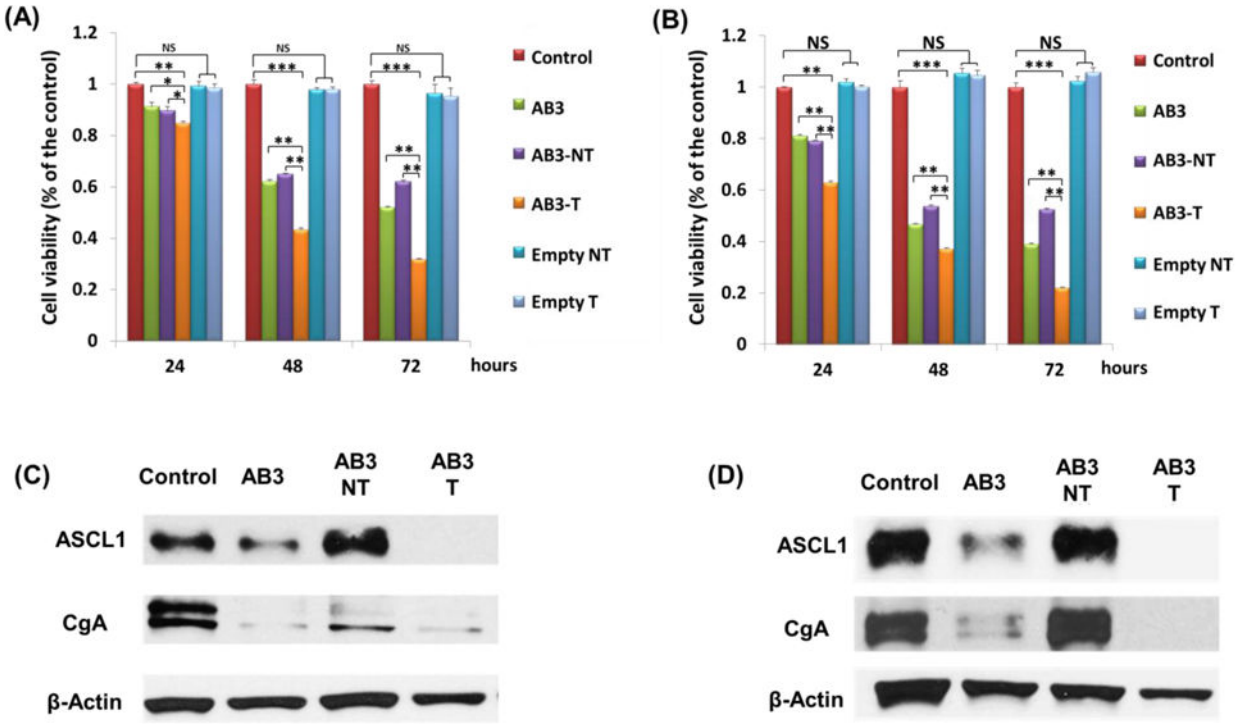

Figure 5.

MTT assays of the (A) TT and (B) MZ–CRC–1 cells (AB3 concentration: 3 μM) treated with cell culture medium (Control), free AB3, and AB3-loaded non-targeted (AB3-NT) and AB3-loaded targeted (AB3-T) micelles. AB3-loaded targeted micelles (**AB3-T**) were much more effective at suppressing tumor cell proliferation than other treatment groups. All values are presented as a mean ± SD (n = 4). *: $p<0.05$; **: $p<0.01$; ***: $p<0.005$; NS: not significant. Western blot analyses for ASCL-1 and CgA of (C) TT and (D) MZ–CRC–1 cells (AB3 concentration: 3 μM) treated with Control, free AB3, and AB3-NT and AB3-T micelles. AB3-T exhibited the highest efficacy at reducing the MTC markers (i.e., ASCL-1 and CgA).

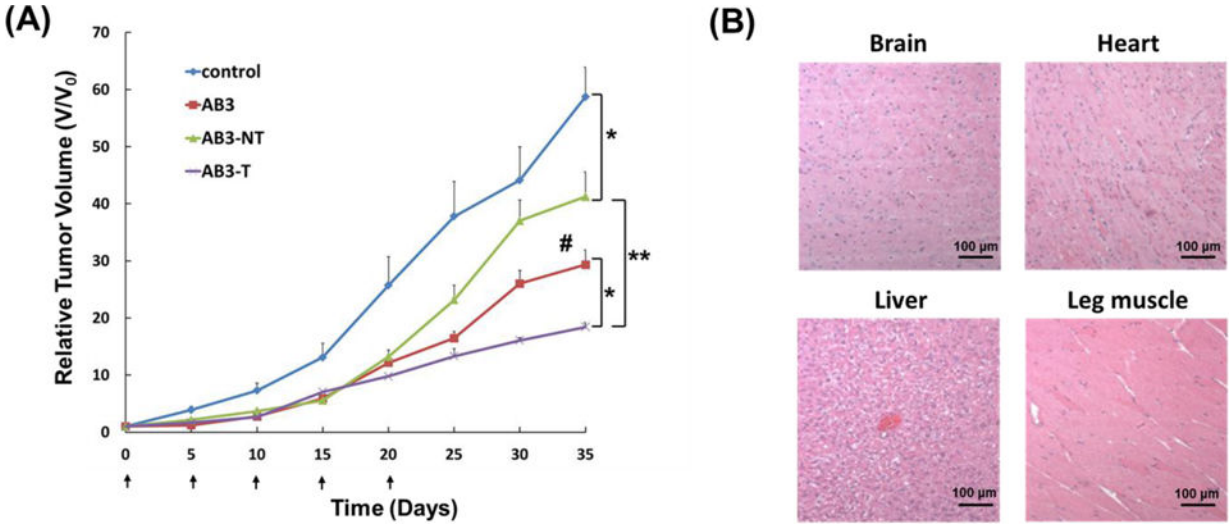

Figure 6.

Therapeutic efficacy of free AB3 and AB3-loaded micelles in subcutaneous TT tumor xenografts. Each mouse received five intravenous injections spaced 5 days apart indicated by the arrows. (A) *In vivo* anticancer efficacy of different AB3 formulations in TT-tumor xenografts. All values are presented as a mean ± SD (n = 6). *: $P < 0.05$; **: $P < 0.01$; NS: not significant. #: Three mice died in the AB3 group due to its severe toxicity. (B) Representative H&E-stained sections of brain, heart, liver, and leg muscles of a mouse treated with AB3-T.